Influence of Urotropin on the Precipitation of Iron Oxides from FeCl 3 Solutions

Šarić, Ankica; Musić, Svetozar; Nomura, Kiyoshi; Popović, Stanko

Source / Izvornik: **Croatica Chemica Acta, 1998, 71, 1019 - 1038**

Journal article, Published version
Rad u časopisu, Objavljena verzija rada (izdavačev PDF)

Permanent link / Trajna poveznica: https://urn.nsk.hr/urn:nbn:hr:217:989462

CROATICA CHEMICA ACTA CCACAA **71** (4) 1019–1038 (1998)

ISSN-0011-1643
CCA-2545 *Original Scientific Paper*

Influence of Urotropin on the Precipitation of Iron Oxides from $FeCl_3$ Solutions

Ankica Šarić,[a] *Svetozar Musić,*[a,*] *Kiyoshi Nomura,*[b] *and Stanko Popović*[c]

[a]*Ruđer Bošković Institute, P. O. Box 1016, 10001 Zagreb, Croatia*

[b]*School of Engineering, University of Tokyo, Hongo 7-3-1, Bunkyo-ku, Tokyo, 113 Japan*

[c]*Department of Physics, Faculty of Science, University of Zagreb, P. O. Box 162, 10001 Zagreb, Croatia*

Received February 6, 1998; accepted June 1, 1998

Precipitations of iron oxides from $FeCl_3$ solutions in the presence of urotropin at 90 °C were monitored using the Fourier transform infrared spectroscopy, Mössbauer spectroscopy, X-ray diffraction and transmission electron microscopy. Urotropin was used as a generator of OH^- ions. The precipitation processes depended on the concentrations of $FeCl_3$ and urotropin and the time of aging. After 1 day of aging the precipitation systems up to pH ≈ 2, the β-FeOOH phase was precipitated, while in the region of $5 < pH < 6$ the mixtures of β-FeOOH, α-Fe_2O_3 and α-FeOOH were precipitated, and at $pH > 6$ the mixtures of α-Fe_2O_3 and α-FeOOH were observed. The β-FeOOH phase precipitated at $2.16 < pH < 5.55$ dissolved after 7 days, yielding soluble iron for the α-FeOOH growth on account of α-Fe_2O_3. At pH ≈ 1.5 and less, β-FeOOH was present as a single phase up to 7 days of aging the precipitation systems. The mechanisms of iron oxide precipitation in dependence on pH were discussed. The size and morphology of oxide particles were strongly influenced by experimental conditions of the precipitation process as shown by transmission electron microscopy.

This article is dedicated to Professor Egon Matijević on the occasion of his 75th birthday.

* Author to whom correspondence should be addressed.

INTRODUCTION

The precipitation chemistry of iron hydroxides, oxyhydroxides and oxides has been the subject of numerous investigations. In publications, these compounds are often described by the term iron oxides (or Fe-oxides), as a group name. Iron oxides were often used as model systems in general studies of colloid and surface properties of metal oxides because they can be prepared as very stable sols and owing to their desirable acid/base behavior at the metal oxide/H_2O interface. The kinetics and mechanisms of crystallization from iron(III)-hydroxide, as well as the phase transformations of iron (III)-oxyhydroxides in aqueous suspensions, were also investigated from various standpoints.

The physico-chemical conditions of iron oxide precipitation may significantly modify the properties of the obtained precipitate, and in some cases the phase composition of the precipitate may be completely changed. For this reason, researchers and engineers focused their attention on the relations between physico-chemical conditions of the iron oxide precipitation, on the one hand, and their surface and bulk properties, on the other. These investigations are important for chemical technology, because iron oxides find many applications as pigments, catalysts, magnetic recording media, gas sensors, *etc.*

In general, iron oxides can be precipitated (a) by slow or forced hydrolysis of Fe(III)-salt solution, (b) by addition of alkali to Fe(III)-salt solution and crystallization from amorphous $Fe(OH)_3$ gel, and (c) by oxidation of Fe(II)-salt solution at various pH values. The phase composition and properties of the precipitate depend on the type of iron salt. As part of our research, we carried out experiments using the $FeCl_3$ salt and urotropin (hexamethylenetetramine). Before presenting our results, we shall focus attention on some selected achievements in this field.

Akaganéite (β-FeOOH) is a typical solid product of slow or forced hydrolysis of $FeCl_3$ solutions.[1] One of the properties of β-FeOOH colloids is the ability to form Schiller layers, which exhibit brilliant interference colors. β-FeOOH possesses a hollandite-type structure with small channels parallel to the *c* axis, which contain water molecules and small amounts of chlorides.[2,3] Ellis *et al.*[4] could not completely wash out chlorides from β-FeOOH particles, so they estimated that less than ≈2% of chlorides is always present in β-FeOOH particles. Paterson and Rahman[5] tried to replace chlorides by perchlorate ions in β-FeOOH microcrystals. However, the replacement of chlorides by perchlorate ions in β-FeOOH channels was not observed. The small amounts of perchlorates substituted for chlorides were associated with protonated surface sites on β-FeOOH microcrystals. The thixotropic behavior of β-FeOOH particles was investigated using the Mössbauer effect.[6]

Holm *et al.*[7] found that the mineral akaganéite is the main solid crystallizing during oxidation of hydrothermal brines. It was suggested that akaganéite had an important role in prebiotic formation of organic substances on earth.

Hamada and Matijević[8] used forced hydrolysis of $FeCl_3$ in ethanol/water solvent to prepare cubic-type hematite (α-Fe_2O_3) particles. Monodispersed β-FeOOH or α-Fe_2O_3 particles were obtained[9] by forced hydrolysis of $FeCl_3$ in ethylene glycol / water solvent. The presence of phosphate ions influenced the morphology and size of precipitated solids in aqueous, as well as in ethylene glycol / water solutions. Addition of phosphate ions favored the formation of ellipsoidal particles. Kandori *et al.*[10] prepared diamond- and spherical-shaped α-Fe_2O_3 particles by forced hydrolysis of acidic $FeCl_3$ solutions. Microstructural investigations of these particles showed that spherical particles were polycrystalline, while diamond-shaped particles were highly crystallized. Morales *et al.*[11] also used forced hydrolysis of $FeCl_3$ solutions in the presence of phosphate anions to prepare monodispersed α-Fe_2O_3 particles of varying axial ratios. The phase transformation, β-FeOOH $\rightarrow$ α-Fe_2O_3, was interpreted by the dissolution/reprecipitation mechanism.[12]

Ozaki *et al.*[13] prepared spindle-type α-Fe_2O_3 particles of narrow size distribution using two procedures. In the first procedure, aqueous or ethanol/water solutions of $FeCl_3$ salt, containing also phosphate or hypophosphite ions, were aged at 100 °C for varying periods of time. The second procedure consisted of (a) $Fe(OH)_3$ precipitation from $Fe(NO_3)_3$ solutions, (b) addition of the HCl + PO_4^{3-} solution to the $Fe(OH)_3$ gel, and (c) aging of the precipitation system at 100 °C. Ozaki and Matijević[14] also prepared spindle-type maghemite (γ-Fe_2O_3) particles by conversion of α-Fe_2O_3 particles of the same shape *via* magnetite (Fe_3O_4).

Small organic ions (citrate, tartarate, oxalate, *etc.*) may significantly influence the process of iron oxide precipitation. For example, Kandori *et al.*[15] investigated the effects of citrate ions on the formation of β-FeOOH and goethite (α-FeOOH). Crystallization of both oxyhydroxide forms was inhibited by citrate ions and the particle size of oxyhydroxide decreased with the increase in the concentration of citrate ions. The effects of citrate ions were more pronounced for β-FeOOH than α-FeOOH, and this was explained by different pH values of precipitation, *i.e.*, β-FeOOH particles crystallized in acidic pH, while α-FeOOH particles crystallized at pH $\approx$ 12. Reeves and Mann[16] investigated the influence of various inorganic anions and organic molecules on forced hydrolysis of $FeCl_3$ salt. In the presence of phosphate ions spindle-type α-Fe_2O_3 particles were obtained. Sulphate ions behaved in a similar manner, but the effect on the shape of α-Fe_2O_3 particles was less pronounced. Organic phosphorus anions showed an increased inhibitory ef-

fect on the hydrolytic reaction compared with inorganic anions of the same concentration. In dependence on the type of organic phosphorus anion, lepidocrocite (γ-FeOOH), β-FeOOH or α-Fe_2O_3 were obtained in the precipitate.

Giant molecules, such as various organic polymers, influenced the crystal growth and morphology of iron oxides in the precipitation systems mainly due to the stereochemical factors. Musić *et al.*[17] investigated forced hydrolysis of $FeCl_3$ in the presence of sodium polyanetholsulphonate. Spherical β-FeOOH particles of micron dimensions were obtained.

In earlier works[18,19] we investigated the precipitation of iron oxide phases, using forced hydrolysis of 0.1 M $FeCl_3$ solution and urotropin. Urotropin was used as a generator of OH^- ions. It is well-known that urotropin generates OH^- ions in acidic medium at elevated temperature in accordance with the chemical reactions:

$$(CH_2)_6N_4 + 6H_2O \rightarrow 4NH_3 + 6HCHO \quad (1)$$

and

$$NH_3 + H_2O \rightarrow NH_4^+ + OH^- \quad (2)$$

β-FeOOH particles were the solid product of $FeCl_3$ hydrolysis. After 5 hours of aging and for an initial 0.025 M urotropin concentration, acicular β-FeOOH particles (monodispersed) of reduced size were obtained. At an initial concentration of 0.25 M urotropin, the particles were amorphous in X-ray diffraction, while Mössbauer spectroscopy indicated that these particles were actually of very small dimensions (superparamagnetic) and probably of the FeOOH structure. After 7 days of aging and at an initial urotropin concentration up to 0.025 M, β-FeOOH was also obtained as a single phase, whereas for $c \geq 0.1$ M mixtures of α-FeOOH and α-Fe_2O_3 were produced. It can be also mentioned here that Matsuda[20] used urotropin in the synthesis of Fe_3O_4 with initial reactants β-FeOOH and $FeCl_2 \cdot 4H_2O$. The reaction was performed at 94 °C and completed in 5 hours. In order to obtain more information about the forced hydrolysis of $FeCl_3$ solutions in the presence of urotropin, we extended our previous investigations[18,19] by varying the concentrations of $FeCl_3$ and the values of other parameters influencing the precipitation process.

EXPERIMENTAL

$FeCl_3 \cdot 6H_2O$, urotropin of analytical grade purity and doubly distilled water were used for the preparation of samples. Chemical composition of the solutions and experimental conditions for the preparation of samples are given in Table I. Total volume of each precipitation system was 200 ml. Aging of the precipitation systems

TABLE I

Experimental conditions for the preparation of samples

Sample	[$FeCl_3$] / M	[Urotropin] / M	Time of aging	pH (final)
C1	0.005	0.025	24 h	7.61
C2	0.010	0.025	24 h	6.51
C3	0.020	0.025	24 h	5.55
C4	0.050	0.025	24 h	1.63
C5	0.300	0.025	24 h	0.78
C6	0.005	0.025	7 d	7.39
C7	0.010	0.025	7 d	6.67
C8	0.020	0.025	7 d	5.29
C9	0.050	0.025	7 d	1.57
C10	0.300	0.025	7 d	0.80
C11	0.005	0.100	24 h	7.74
C12	0.010	0.100	24 h	6.80
C13	0.020	0.100	24 h	6.37
C14	0.050	0.100	24 h	5.10
C15	0.300	0.100	24 h	0.94
C16	0.005	0.100	7 d	7.83
C17	0.010	0.100	7 d	7.36
C18	0.020	0.100	7 d	6.81
C19	0.050	0.100	7 d	6.00
C20	0.300	0.100	7 d	1.00
C21	0.005	0.250	24 h	7.76
C22	0.010	0.250	24 h	7.07
C23	0.020	0.250	24 h	6.78
C24	0.050	0.250	24 h	6.16
C25	0.300	0.250	24 h	2.16
C26	0.005	0.250	7 d	8.36
C27	0.010	0.250	7 d	8.07
C28	0.020	0.250	7 d	7.98
C29	0.050	0.250	7 d	7.30
C30	0.300	0.250	7 d	4.95

was performed in glass autoclaves at 90 °C. After a proper aging time, solid hydrolytical products were separated from the mother liquor using an ultraspeed centrifuge (operational range up to 20000 r.p.m.). The solid hydrolytical products were subsequently washed with doubly distilled water. Microstructural characterizations of the samples were performed by the Fourier transform infrared (FT-IR) spectroscopy, X-ray diffraction Mössbauer spectroscopy and transmission electron microscopy (TEM).

The FT-IR spectra were recorded using a Perkin-Elmer spectrometer 2000 model. The IRDM (Infrared Data Manager) program, obtained by Perkin-Elmer, was used to process the recorded spectra.

Mössbauer spectra were recorded using standard equipment and a ^{57}Co source. Mathematical deconvolutions of the recorded spectra were performed using a standard procedure.

X-ray powder diffraction measurements were performed using the Philips diffractometer MPD 1880 model (Cu-Kα radiation, graphite monochromator and proportional counter).

The size and shape of the particles were monitored by transmission electron microscopy (Opton EM-10 model). Before the transmission electron microscopic observation, the powders were dispersed in doubly distilled water by ultrasonic waves and then a drop of the dispersion was placed on a copper grid, previously covered by a polymer film.

RESULTS AND DISCUSSION

FT-IR Spectroscopy

The present work shows high potentials of FT-IR spectroscopy in monitoring phase changes in the iron oxide precipitates. This is illustrated by the FT-IR spectra shown in Figures 1 to 6.

Figures 1 and 2 show the FT-IR spectra of samples C1 to C10, prepared by varying the concentration of $FeCl_3$, and at an initial concentration of 0.025 M urotropin. After 24 hours of aging the precipitation system, prepared from 0.005 M $FeCl_3$ solution, a mixture of α-Fe_2O_3 and α-FeOOH was observed. The IR bands at 563 and 464 cm^{-1} are due to the presence of α-Fe_2O_3, whereas the bands at 896 and 799 cm^{-1} are typical of α-FeOOH. At a concentration of 0.02 M $FeCl_3$, the β-FeOOH phase appeared in sample C3, as concluded on the basis of a new and strong IR band at 694 cm^{-1}. The origin of IR bands corresponding to α-FeOOH, β-FeOOH and α-Fe_2O_3 will not be discussed here because adequate assignations of these IR bands were presented in earlier papers.[18,21–23] At concentrations of 0.05 and 0.3 M $FeCl_3$, the presence of β-FeOOH, as a single phase in samples C4 and C5, is observed. These phase changes in the precipitates were associated with the pH change in the mother liquor from 7.61 to 0.78. After 7 days of aging the precipitation systems C6 to C10, the main change was observed in the FT-IR spectrum of sample C8, precipitated from 0.02 M $FeCl_3$. The fraction of the α-FeOOH phase (IR bands at 896 and 800 cm^{-1}) significantly increased, whereas the β-FeOOH phase was absent. The pH of the mother liquor decreased from 5.55 to 5.29. This shows that the fraction of β-FeOOH, formed at the beginning of the precipitation process, dissolved after 7 days.

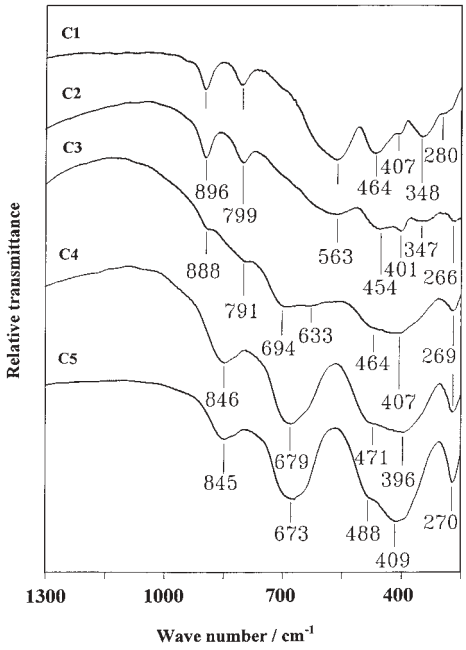

Figure 1. FT-IR spectra of samples C1-C5, recorded at room temperature.

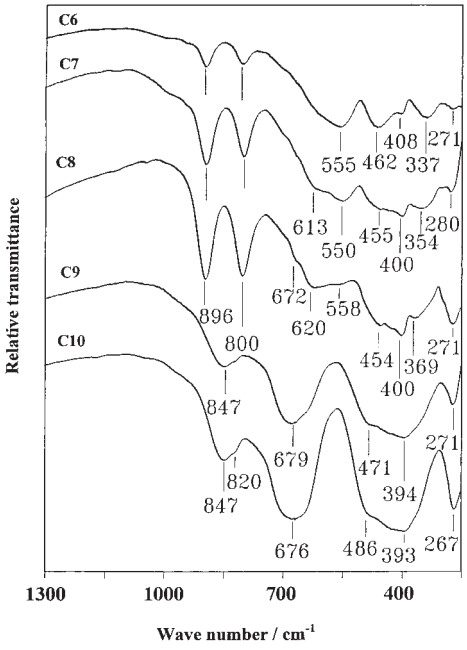

Figure 2. FT-IR spectra of samples C6-C10, recorded at room temperature.

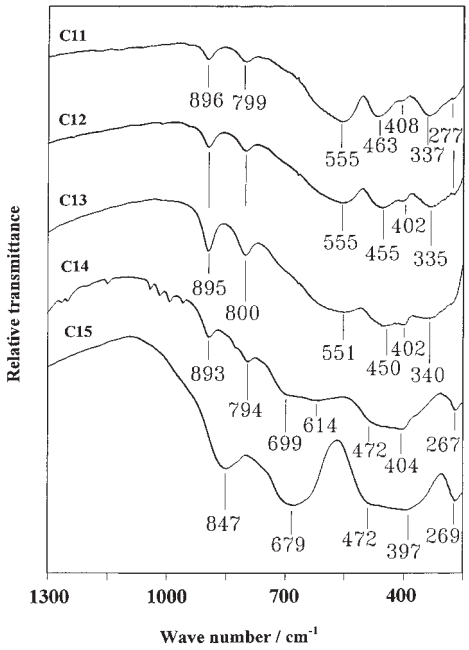

Figure 3. FT-IR spectra of samples C11-C15, recorded at room temperature.

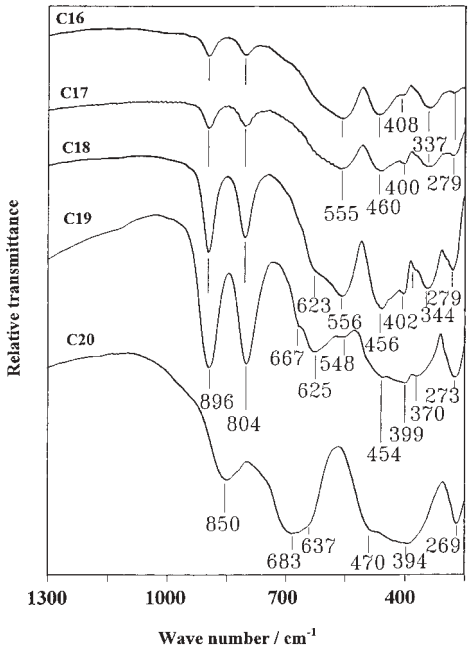

Figure 4. FT-IR spectra of samples C16-C20, recorded at room temperature.

Figures 3 and 4 show the FT-IR spectra of samples C11 to C20, precipitated from the $FeCl_3$ solutions with an initial urotropin concentration of 0.1 M. At concentrations up to 0.02 M $FeCl_3$, mixtures of α-Fe_2O_3 and α-FeOOH were obtained (samples C11, C12 and C13), whereas at a concentration of 0.05 M $FeCl_3$, a mixture of β-FeOOH, α-Fe_2O_3 and α-FeOOH was obtained, similarly as in the case of sample C3. The FT-IR spectrum of sample C15 can be assigned to β-FeOOH. After 7 days of aging the precipitation system C14, the α-FeOOH fraction significantly increased (IR bands at 896 and 804 cm^{-1}).

Figures 5 and 6 show the FT-IR spectra of samples C21 to C30, precipitated from the $FeCl_3$ solutions with an initial urotropin concentration of 0.25 M. For concentrations up to 0.05 M $FeCl_3$ and 24 hours of aging of the precipitation systems, mixtures of α-Fe_2O_3 and α-FeOOH were found, whereas the β-FeOOH phase was obtained for the concentration of 0.3 M $FeCl_3$. After 7 days of aging, the β-FeOOH phase dissolved, so the dominant phase in sample C30 was α-FeOOH (IR bands at 896, 800, 633 cm^{-1}), and the minor phase was α-Fe_2O_3 (IR shoulders at 573 and 454 cm^{-1}).

On the basis of the above-presented results, a general rule on the precipitation of iron oxides from $FeCl_3$ solutions, in the presence of urotropin, was established. After 24 hours of aging the precipitation systems in the pH region up to ≈ 2, the β-FeOOH is produced as a single phase, in the region $5 < pH < 6$ mixtures of β-FeOOH, α-Fe_2O_3 and α-FeOOH are produced, while at $pH > 6$ mixtures of α-Fe_2O_3 and α-FeOOH are observed. With a prolonged time of aging (7 days) the precipitation systems, β-FeOOH, formed at $2.16 < pH < 5.55$, was dissolved giving the feeding material for α-FeOOH growth on account of α-Fe_2O_3. At $pH \leq 1.5$, β-FeOOH was found to precipitate as a single phase up to 7 days. At the early stage of the $FeCl_3$ hydrolysis, formation of hydroxy complexes and polymers of Fe^{3+} ions occurs. In these hydroxy polymers, OH^- groups are partially substituted for chlorides.[24] With an increase in pH, caused by chemical decomposition of urotropin, there is strong competition between OH^- and Cl^- ions, and with a prolonged time of aging Cl^- ions are almost completely eliminated from the solid hydrolytical product. Only residual Cl^- ions (up to ≈ 2%) are present[4] due to the specific structure of β-FeOOH.

Mössbauer Spectroscopy

Mössbauer spectroscopy has found an important application in the investigation of iron oxides.[25] For this reason, we have also applied this technique in the investigation of our samples to obtain additional information about the nature of these samples. Typical results obtained by Mössbauer spectroscopy are summarized in Figures 7, 8 and 9, and in Table II.

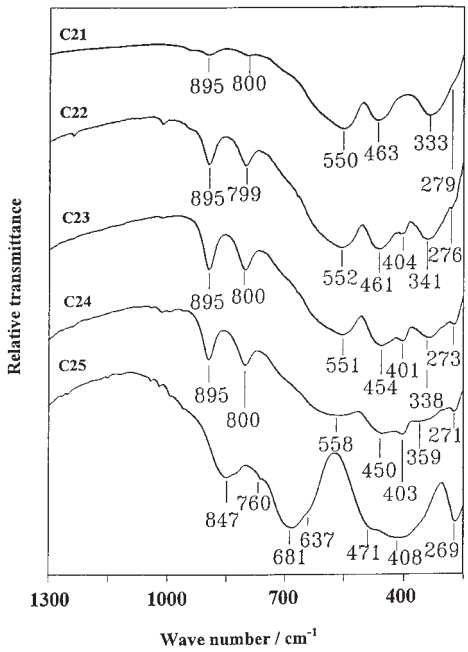

Figure 5. FT-IR spectra of samples C21-C25, recorded at room temperature.

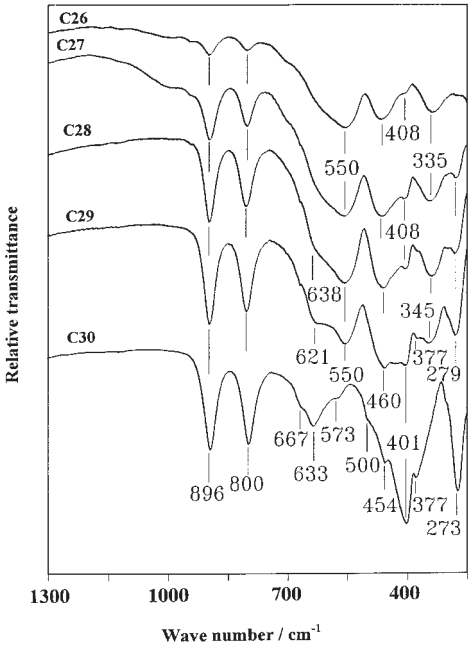

Figure 6. FT-IR spectra of samples C26-C30, recorded at room temperature.

The RT Mössbauer spectra of samples C5, C20 and C30 are shown in Figure 7. These samples were precipitated from 0.3 M $FeCl_3$ solutions with varying concentrations of urotropin. The spectra of samples C5 and C20

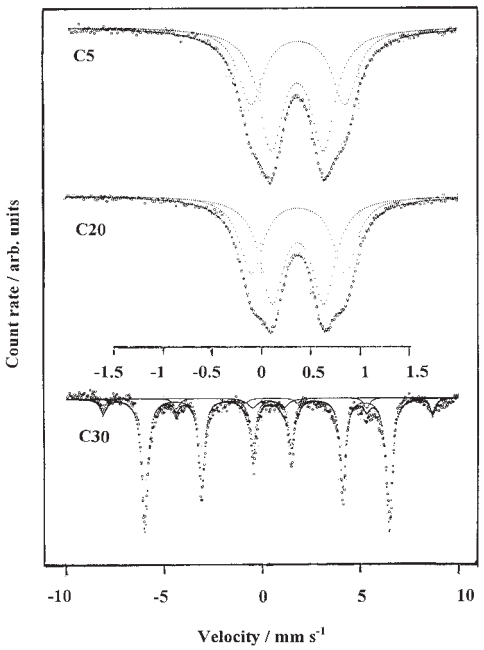

Figure 7. ^{57}Mössbauer spectra of samples C5, C20 and C30, recorded at room temperature.

were considered as the superposition of two quadrupole doublets and they can be ascribed to β-FeOOH. In an earlier work,[26] β-FeOOH was prepared by slow hydrolysis of 0.1 M $FeCl_3$ solution and the Mössbauer spectrum at RT of this sample showed the superposition of two quadrupole doublets having the following parameters: $\Delta_1 = 0.532$ and $\Delta_2 = 0.884$ mm s^{-1}, $\Gamma_1 = 0.256$ and $\Gamma_2 = 0.297$ mm s^{-1}. The area under the peaks of doublet Q_1 was 61.44%, while the isomer shifts of $\delta_1 = 0.381$ and $\delta_2 = 0.393$ mm s^{-1} (relative to α-Fe) were similar. These results clearly indicated the presence of two kinds of iron atoms contributing to the Mössbauer effect in β-FeOOH. Several researchers tried to interpret the nature of the two doublets in the Mössbauer spectrum of β-FeOOH. For example, Johnston and Logan[27] suggested that the inner doublet in the Mössbauer spectrum of β-FeOOH is a consequence of iron in the structural $O_3(OH)_3$ octahedron, whereas the outer doublet is a

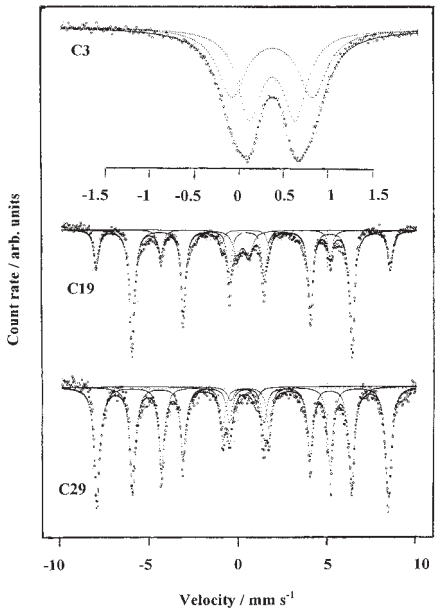

Figure 8. ^{57}Mössbauer spectra of samples C3, C19 and C29, recorded at room temperature.

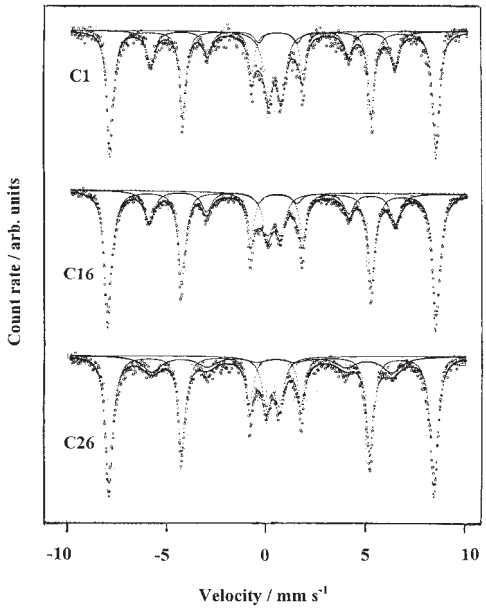

Figure 9. ^{57}Mössbauer spectra of samples C1, C16 and C26, recorded at room temperature.

TABLE II

^{57}Fe Mössbauer parameters of selected samples as calculated on the basis of the spectra recorded at room temperature

Sample	Spectral component	δ / mm s^{-1}	Δ or E_q / mm s^{-1}	HMF / T	Γ / mm s^{-1}	A / %
C5	Q_1	0.37	0.53		0.30	59.6
	Q_2	0.38	0.95		0.31	40.4
C20	Q_1	0.37	0.52		0.29	57.0
	Q_2	0.38	0.95		0.29	43.0
C30	Q	0.31	1.57			24.0
	S_1	0.37	0.27	38.6	0.37	68.2
	S_2	0.40	0.16	51.9	0.36	7.8
C3	Q_1	0.37	0.51		0.32	52.2
	Q_2	0.37	0.91		0.38	47.8
C19	Q	0.28	0.66		0.54	40.6
	S_1	0.37	0.27	38.4	0.33	45.5
	S_2	0.36	0.11	51.2	0.32	13.9
C29	Q	0.31	1.43		0.45	17.6
	S_1	0.37	0.27	38.3	0.38	38.4
	S_2	0.37	0.16	50.9	0.37	44.0
C1	Q	0.35	0.66		0.54	60.1
	S_1	0.38	0.26	38.0	0.51	10.5
	S_2	0.37	0.20	50.8	0.39	29.4
C16	Q	0.34	0.65		0.60	46.8
	S_1	0.37	0.26	38.3	0.59	12.4
	S_2	0.37	0.21	51.2	0.43	40.8
C26	Q	0.33	0.66		0.55	48.0
	S_1	0.37	0.26	37.6	1.16	12.0
	S_2	0.37	0.20	50.7	0.43	40.0

δ = isomer shift given relative to α-Fe
Δ = quadrupole splitting of doublet Q
E_q = quadrupole splitting of sextet S
HMF = hyperfine magnetic field
Γ = line-width
A = area under the peaks.

Errors: δ, Δ and E_q = 0.01 mm s^{-1}, HMF = $\pm$ 0.2 T.

consequence of iron in the tunnels, *i.e.*, the chain of cavities along the *c* axis of the hollandite-like structure. Childs *et al.*[28] suggested that iron in the $O_3(OH)_3$ octahedron is responsible for the inner doublet, whereas iron in $O_2(OH)_4$ octahedron is responsible for the outer doublet. This conclusion was supported by Chambaere *et al.*[29] The outer doublet in the Mössbauer spectrum of β-FeOOH was also discussed[30] in terms of chlorine-substituted octahedron, $O_3(OH)_2Cl$. Murad[31] recorded Mössbauer spectra of β-FeOOH at 135 and 4 K. These spectra could be resolved into at least three superimposed sextets corresponding to various Fe^{3+} sites in β-FeOOH. For the β-FeOOH spectrum recorded at 4 K the following parameters were calculated: $\delta_1 = 0.36$, $Eq_1 = 0.90$, $HMF_1 = 47.3$; $\delta_2 = 0.35$, $Eq_2 = 0.30$, $HMF_2 = 47.9$ and $\delta_3 = 0.37$ mm s^{-1}, $Eq_3 = -0.05$ mm s^{-1}, $HMF_3 = 48.6$ T, respectively.

The RT Mössbauer spectrum of sample C30 showed that α-FeOOH is the dominant phase in this sample. Also, a small amount of α-Fe_2O_3 was calculated on the basis of the outer sextet. The quadrupole doublet Q of sample C30, as shown in Table II, is introduced to improve the fitting procedure. However, the central quadrupole doublet observed in the same spectrum could not be fitted because of its low intensity.

The RT Mössbauer spectra of samples C3, C19 and C29 are shown in Figure 8. The spectrum of sample C3 was characterized by the parameters that can be ascribed to β-FeOOH. The spectrum of the same sample, recorded at higher velocities, did not show the HMF component. The spectra of samples C19 and C29 showed that in sample C19 the dominant phase is α-FeOOH (the inner sextet), whereas in sample C29 near equal amounts of α-Fe_2O_3 and a-FeOOH are observed.

The RT Mössbauer spectra of samples C1, C16 and C26 are shown in Figure 9. These spectra indicate that α-Fe_2O_3 (outer sextet) is the dominant phase in these samples, whereas α-FeOOH (inner sextet) is the minor phase. The quadrupole splitting of central quadrupole doublet, $\Delta \approx 0.65$ mm s^{-1}, observed in these spectra, could be ascribed to β-FeOOH; however, it is more likely that the origin of this doublet is due to the fraction of superparamagnetic particles.

X-ray Diffraction

The results of phase analysis of selected samples, as determined by the X-ray powder diffraction, are given in Table III. XRD indicates that sample C1 is a mixture of α-Fe_2O_3 as the dominant phase and α-FeOOH as the minor phase. In samples C3 and C5, the β-FeOOH phase was detected, and the diffraction lines of sample C3 were very broad. XRD also indicated the influence of pH on the phase composition of the precipitates, for example, in

TABLE III

The results of phase analysis of selected samples, as determined by X-ray powder diffraction

Sample	Phase composition	Remark	Crystallite size /nm
C1	α-Fe_2O_3 (dominant) α-FeOOH		
C3	β-FeOOH	VBDL	not measurable
C5	β-FeOOH		
C16	α-Fe_2O_3 (dominant) α-FeOOH		
C19	α-FeOOH (dominant) α-Fe_2O_3		
C20	β-FeOOH	BDL	8 ± 1
C26	α-Fe_2O_3 (dominant) α-FeOOH		
C29	α-FeOOH α-Fe_2O_3		
C30	α-FeOOH (dominant) α-Fe_2O_3		

BDL = broadened diffraction lines (small crystallite sizes)
VBDL = very broadened diffraction lines (very small crystallite sizes).

sample C16 precipitated at pH = 7.83, the α-Fe_2O_3 phase was dominant, in sample C19 precipitated at pH = 6.00, the α-FeOOH phase was dominant and in sample C20 precipitated at pH = 1.00, the β-FeOOH was obtained as a single phase. The crystallite size of β-FeOOH in sample C20 was 8 nm, as determined using the Scherrer equation. XRD results, obtained for samples C26, C29 and C30, are comparable to the FT-IR and Mössbauer spectroscopic results.

Transmission Electron Microscopy (TEM)

Morphologies of the particles were investigated by transmission electron microscopy. Transmission electron images of selected samples are summarized in Figures 10, 11 and 12, and they indicate how strongly the size and morphology of iron oxide particles are influenced by the experimental conditions of their precipitation.

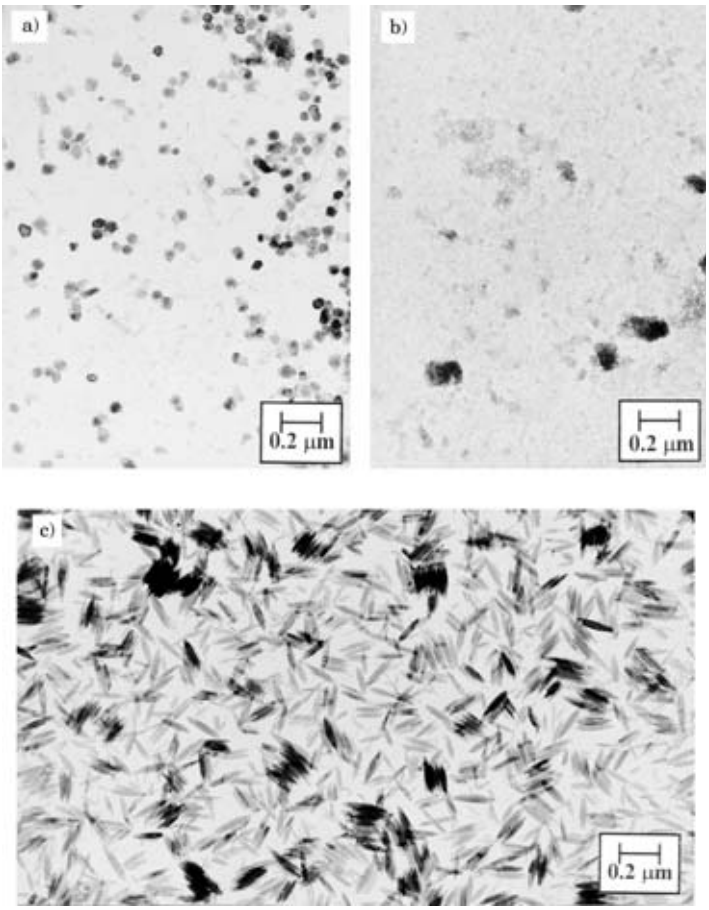

Figure 10. TEM images of (a) sample C1, (b) sample C3 and (c) sample C5.

The image of sample C1 (Figure 10) shows α-Fe_2O_3 particles and α-FeOOH needles of varying length. Very small particles are visible in sample C3 and this agrees with XRD, which for this sample (β-FeOOH) showed wery broad diffraction lines. β-FeOOH present in sample C5 showed spindle--type β-FeOOH particles showing a tendency to lateral arraying. Urotropin strongly controls changes in the particle morphology. The image of sample C19 (Figure 11) shows α-FeOOH needles as dominant particles and α-Fe_2O_3 polyhedra in minor concentrations. On the other hand, the image of sample C29, compared with the image of sample C19, shows α-FeOOH and α-Fe_2O_3 particles at almost equal concentrations and a marked decrease in the size of particles. Small β-FeOOH particles are visible in the image of sample C20; however, they are significantly greater than those of β-FeOOH in sample

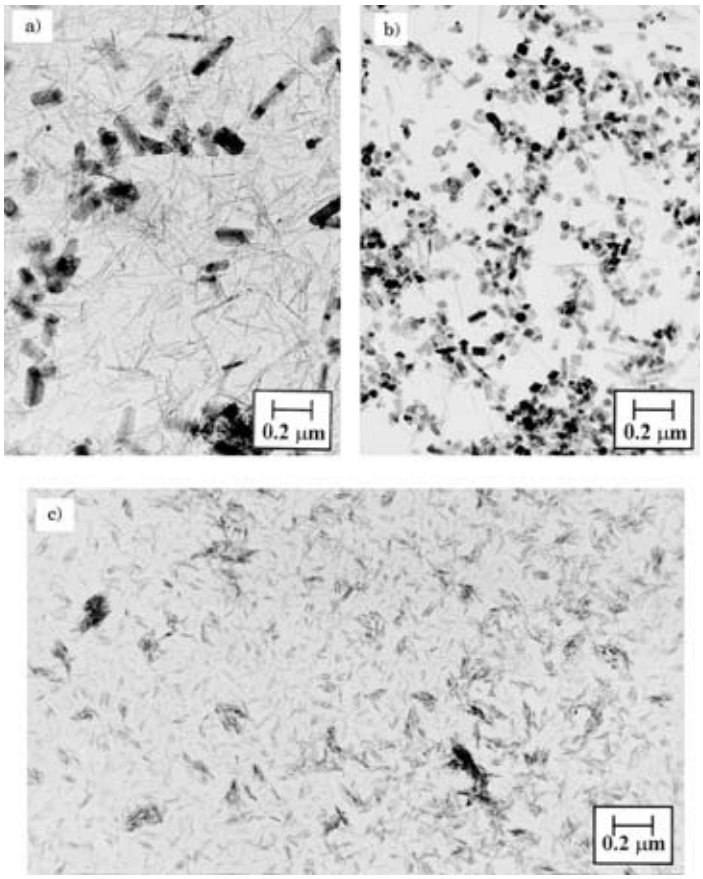

Figure 11. TEM images of (a) sample C19, (b) sample C29 and (c) sample C20.

C3. The image of sample C30 (Figure 12) shows the presence of dendrite-type α-FeOOH particles, α-Fe_2O_3 polyhedra and needle-type particles.

CONCLUSIONS

Precipitation of iron oxides from $FeCl_3$ solutions, in the presence of urotropin at 90 °C, is a complex process which depends on the concentrations of $FeCl_3$ and urotropin and the time of aging the precipitation system. Urotropin undergoes chemical decomposition in acidic medium at elevated temperature, thus generating OH^- ions.

The concentrations of $FeCl_3$ varied from 0.005 to 0.3 M, and those of urotropin from 0.025 to 0.25 M. On the basis of analyses of the precipitates by

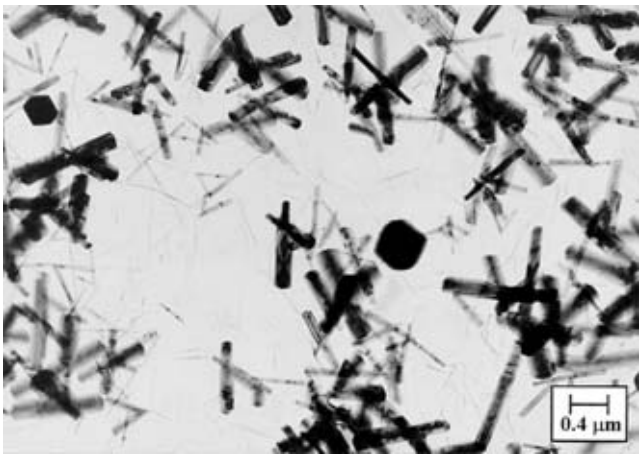

Figure 12. TEM image of sample C30.

FT-IR spectroscopy, Mössbauer spectroscopy and X-ray diffraction, it was possible to summarize the effects of urotropin on the precipitation of iron oxides from $FeCl_3$ solutions. After 1 day of aging the precipitation system up to pH ≈ 2, the β-FeOOH phase was precipitated, while in the region 5 < pH < 6 the mixtures of β-FeOOH, α-Fe_2O_3 and α-FeOOH were precipitated, and at pH > 6 mixtures of α-Fe_2O_3 and α-FeOOH were observed. The β-FeOOH phase precipitated at 2.16 < pH < 5.55 dissolved after 7 days, yielding soluble iron for the α-FeOOH growth on account of α-Fe_2O_3. At pH ≈ 1.5 and less, β-FeOOH was present as a single phase up to 7 days of aging the precipitation system.

At an early stage of $FeCl_3$ hydrolysis, formation of hydroxy complexes and polymers of Fe ions occurs. In these hydroxy polymers, OH^- groups are partially substituted for chlorides. Chemical decomposition of urotropin increases the pH, thus inducing strong competition between OH^- and Cl^- ions, and with a prolonged time of aging, chlorides are almost completely eliminated from the solid hydrolytic product. The increase in the pH created conditions for the formation of α-FeOOH and α-Fe_2O_3.

In the absence of urotropin, the hydrolysis of acidic $FeCl_3$ solutions produced β-FeOOH, which under suitable conditions in the suspension may convert to α-Fe_2O_3 by the dissolution/reprecipitation mechanism. On the other hand, in high alkaline medium two different and competitive mechanisms[32] are involved in the crystallization process from ferrihydrite. It is suggested that α-FeOOH crystals growth from Fe^{3+} ions is generated by dissolution of ferrihydrite, whereas α-Fe_2O_3 forms *via* internal dehydration and rearrangement within the ferrihydrite aggregates. Conversion of β-FeOOH

to α-FeOOH and/or α-Fe_2O_3 in alkaline medium was also monitored,[33] and it was concluded that this process proceeds by the dissolution/reprecipitation mechanism.

The present work also shows that the size and morphology of iron oxide particles are strongly influenced by experimental conditions of the precipitation process. β-FeOOH particles showed spindle- and rod-like morphologies. α-FeOOH needles and dendrites and α-Fe_2O_3 polyhedra were also observed.

Acknowledgment. – The authors wish to thank Professor Nikola Ljubešić for his assistance in electron microscopy.

REFERENCES

1. H. Maeda and Y. Maeda, *Langmuir* **12** (1996) 1446–1452.
2. S. T. Galbraith, T. Baird, and J. R. Fryer, *An investigation of the dehydration of β-iron oxyhydroxide*, Inst. Phys. Conf. Ser. No. 52 C, Chapter 5, 1980, pp. 291–294.
3. N. G. Holm, *Origins of Life* **15** (1985) 131–139.
4. J. Ellis, R. Giovanoli, and W. Stumm, *Chimia* **30** (1976) 194–197.
5. R. Paterson and H. Rahman, *J. Colloid. Interface Sci*. **97** (1984) 423–427.
6. D. Hanžel and F. Sevšek, *J. Physique C6* **37** (1976) 277–279.
7. N. G. Holm, T. Wadsten, and M. J. Dowler, *Estud. Geol*. **38** (1982) 367–371.
8. S. Hamada and E. Matijević, *J. Chem. Soc., Faraday Trans. I* **78** (1982) 2147–2156.
9. E. Matijević and Š. Cimaš, *Colloid. Polym. Sci*. **265** (1987) 155–163.
10. K. Kandori, S. Tamura, and T. Ishikawa, *Colloid. Polym. Sci*. **272** (1994) 812–819.
11. M. P. Morales, T. Gonzáles-Carreño, and C. J. Serna, *J. Mater. Res*. **7** (1992) 2538–2545.
12. E. K. De Blanco, M. A. Blesa, and S. J. Liberman, *Reactivity of Solids* **1** (1986) 189–194.
13. M. Ozaki, S. Kratohvil, and E. Matijević, *J. Colloid. Interface Sci.* **102** (1984) 148–151.
14. M. Ozaki and E. Matijević, *J. Colloid Interface Sci*. **107** (1985) 199–203.
15. K. Kandori, M. Fukuoka, and T. Ishikawa, *J. Mater. Sci*. **26** (1991) 3313–3319.
16. N. J. Reeves and S. Mann, *J. Chem. Soc., Faraday Trans*. **87** (1991) 3875–3880.
17. S. Musić, M. Gotić, and N. Ljubešić, *Mater. Lett*. **25** (1995) 69–74.
18. S. Musić, A. Šarić, and S. Popović, *J. Mol. Struct*. **410–411** (1997) 153–156.
19. A. Šarić, K. Nomura, S. Popović, N. Ljubešić, and S. Musić, *Mater. Chem. Phys*. **52** (1998) 214–220.
20. K. Matsuda, *Proceedings of the Faculty of Natural Sciences*, Tokai University **21** (1986) 53–58.
21. J. E. Iglesias and C. J. Serna, *Miner. Petrogr. Acta* **29A** (1985) 363–370.
22. S. Musić, I. Czakó-Nagy, S. Popović, A. Vértes, and M. Tonković, *Croat. Chem. Acta* **59** (1986) 833–851.

23. S. Musić, Z. Orehovec, S. Popović, and I. Czakó-Nagy, *J. Mater. Sci*. **29** (1994) 1991–1998.
24. S. Musić, A. Vértes, G. W. Simmons, I. Czakó-Nagy, and H. Leidheiser, Jr., *J. Colloid. Interface Sci.* **85** (1982) 256–266.
25. A. Vértes, L. Korecz, and K. Burger, *Mössbauer Spectroscopy*, Elsevier Sci. Publ. Co., Amsterdam-Oxford-New York, 1979, 432 pages.
26. M. Gotić, S. Popović, N. Ljubešić, and S. Musić, *J. Mater. Sci.* **29** (1994) 2474–2480.
27. J. H. Johnston and N. E. Logan, *J. Chem. Soc., Dalton Trans*. **13** (1979) 13–16.
28. C. Childs, B. Goodman, E. Paterson, and F. Woodhams, *Aust. J. Chem*. **33** (1980) 15–26.
29. D. G. Chambaere, E. De Grave, R. L. Vanleeberghe, and R. E. Vandenberghe, *Hyperfine Interact*. **20** (1984) 249–262.
30. M. Ohyabu and Y. Ujihira, *J. Inorg. Nucl. Chem*. **43** (1981) 3125–3129.
31. E. Murad, *Clay Miner.* **14** (1979) 273–283.
32. U. Schwertmann and E. Murad, *Clays Clay Miner.* **31** (1983) 277–284.
33. R. M. Cornell and R. Giovanoli, *Clays Clay Miner.* **38** (1990) 469–476.

SAŽETAK

Utjecaj urotropina na taloženje oksida željeza iz otopina $FeCl_3$

Ankica Šarić, Svetozar Musić, Kiyoshi Nomura i Stanko Popović

Taloženje oksida željeza iz otopina $FeCl_3$ u prisutnosti urotropina pri 90 °C proučavana su primjenom FT-IR i Mössbauerove spektroskopije, difrakcije X-zraka i transmisijske elektronske mikroskopije. Urotropin je rabljen kao generator iona OH^-. Taložni procesi ovisili su o koncentracijama $FeCl_3$ i urotropina, te o vremenu starenja. Faza β-FeOOH istaložena je nakon jednog dana starenja taložnog sustava do pH ≈ 2, dok su smjese β-FeOOH, α-Fe_2O_3 i α-FeOOH istaložene u području $5 < pH < 6$, a pri $pH > 6$ dobivene su smjese α-Fe_2O_3 i α-FeOOH. Nakon 7 dana starenja otopljena je faza β-FeOOH, istaložena u području $2{,}16 < pH < 5{,}55$, a nastali (otopljeni) ioni željeza poslužili su prvenstveno za kristalni rast α-FeOOH na račun α-Fe_2O_3. Faza β-FeOOH bila je stabilna do 7 dana starenja taložnog sustava pri pH ≈ 1,5 i niže. Razmotreni su mehanizmi taloženja oksida željeza u ovisnosti o pH. Veličina i morfologija oksidnih čestica jako su ovisili o eksperimentalnim uvjetima taložnog procesa, kao što je prikazano transmisijskom elektronskom mikroskopijom.